

# Structure-Based Design of Potent Small-Molecule Binders to the S-Component of the ECF Transporter for Thiamine

Lotteke J. Y. M. Swier,<sup>[a]</sup> Leticia Monjas,<sup>[b]</sup> Albert Guskov,<sup>[a]</sup> Alrik R. de Voogd,<sup>[b]</sup> Guus B. Erkens,<sup>[a]</sup> Dirk J. Slotboom,<sup>\*[a]</sup> and Anna K. Hirsch<sup>\*[b]</sup>

Energy-coupling factor (ECF) transporters are membrane-protein complexes that mediate vitamin uptake in prokaryotes. They bind the substrate through the action of a specific integral membrane subunit (S-component) and power transport by hydrolysis of ATP in the three-subunit ECF module. Here, we have studied the binding of thiamine derivatives to ThiT, a thiamine-specific S-component. We designed and synthesized derivatives of thiamine that bind to ThiT with high affinity; this allowed us to evaluate the contribution of the functional

groups to the binding affinity. We determined six crystal structures of ThiT in complex with our derivatives. The structure of the substrate-binding site in ThiT remains almost unchanged despite substantial differences in affinity. This work indicates that the structural organization of the binding site is robust and suggests that substrate release, which is required for transport, requires additional changes in conformation in ThiT that might be imposed by the ECF module.

## Introduction

ATP-binding cassette (ABC) transporters are found in all kingdoms of life and are involved in many crucial processes.<sup>[1]</sup> The recently discovered energy-coupling factor (ECF) transporters form a structurally distinct subtype of ABC transporters.<sup>[2,3]</sup> These transporters mediate the uptake of a wide variety of substrates, among which are water-soluble vitamins, cofactors, their precursors, and the transition-metal ions  $\text{Co}^{2+}$  and  $\text{Ni}^{2+}$ .<sup>[4]</sup> ECF transporters are found in prokaryotes, but have not been identified in eukaryotes. In the kingdom of bacteria, the transporters are found in particular in the phylum of the Firmicutes. This phylum includes many human pathogens such as *Staphylococci*, *Streptococci*, *Enterococci*, and *Listeriae*.<sup>[3,5]</sup> These pathogens lack enzymes for the de novo synthesis of many vitamins and cofactors and are dependent on membrane proteins such as the ECF transporters for the uptake of these molecules. Because of their absence in humans, ECF transporters are potential targets for the development of new antibiotics.

ECF transporters feature the basic architecture of ABC transporters, consisting of two cytoplasmic nucleotide-binding domains (NBDs) and two transmembrane domains (Figure 1A).

One of the transmembrane domains is responsible for substrate binding and is termed the S-component. The mode of substrate binding is one of the defining characteristics of ECF transporters, because other ABC transporters that import substrates in prokaryotes invariably make use of soluble extracytoplasmic binding proteins or domains. The identical or similar NBDs of ECF transporters (EcfA and EcfA') bind and hydrolyze ATP. It is hypothesized that the energy released in this process induces changes in conformation within and between the different domains of the transporter, and that this allows transport of the substrate across the membrane. These changes in conformation are thought to be transduced from the NBDs to the S-component and vice versa through the action of the second transmembrane domain, called EcfT. EcfA, EcfA', and EcfT together form the eponymous ECF module.

Although the architectures of three ECF transporters have been revealed recently,<sup>[6–8]</sup> the transport mechanism is not fully elucidated. To investigate this mechanism, we focused on substrate binding to the S-component ThiT from *Lactococcus lactis*. ThiT is a 21-kDa protein that binds its natural substrate thiamine (vitamin B<sub>1</sub>) with sub-nanomolar affinity.<sup>[9]</sup> Thiamine is a precursor of thiamine diphosphate (TDP), which serves as a cofactor in many enzymes that perform decarboxylations and are involved in essential cellular processes.<sup>[10]</sup> TDP and its precursor thiamine monophosphate (TMP) can bind to ThiT as well, but with lower affinities.<sup>[9]</sup> The crystal structure of ThiT from *L. lactis* has been solved previously at 2.0 Å resolution (PDB ID: 3RLB).<sup>[11]</sup>

Here, we rationally designed derivatives of thiamine such that the various moieties of the original thiamine molecule were altered one-by-one, in order to explore the space within the substrate-binding pocket. The aim of this study was to trap the protein in previously undetected conformational

[a] L. J. Y. M. Swier,<sup>†</sup> Dr. A. Guskov, Dr. G. B. Erkens, Prof. D. J. Slotboom  
Groningen Biomolecular Sciences and Biotechnology Institute  
University of Groningen  
Nijenborgh 4, 9747 AG Groningen (The Netherlands)  
E-mail: d.j.slotboom@rug.nl  
Homepage: <http://www.rug.nl/research/membrane-enzymology/>

[b] L. Monjas,<sup>†</sup> A. R. de de Voogd, Dr. A. K. H. Hirsch  
Stratingh Institute for Chemistry, University of Groningen  
Nijenborgh 7, 9747 AG Groningen (The Netherlands)  
E-mail: a.k.h.hirsch@rug.nl  
Homepage: <http://www.rug.nl/research/bio-organic-chemistry/hirsch/>

[<sup>†</sup>] These authors contributed equally to this work.

Supporting information for this article is available on the WWW under <http://dx.doi.org/10.1002/cbic.201402673>.

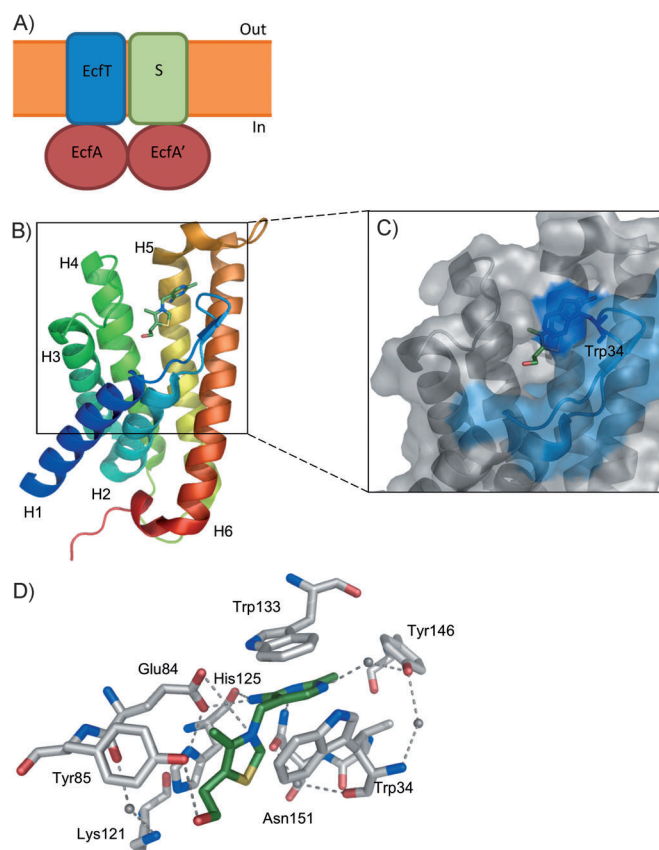


**Figure 1.** Architecture of an ECF transporter and the structure of thiamine-bound ThiT of *L. lactis*. A) Schematic representation of an ECF transporter in which the nucleotide-binding domains EcfA and EcfA' are shown in red, the transmembrane domain EcfT in blue, the S-component in green, and the membrane in orange. The cytoplasmic and extracytoplasmic space are indicated by the words "In" and "Out", respectively. B) Secondary-structure representation of ThiT, colored from the N terminus in blue to the C terminus in red. Helices 1–6 are indicated by H1–H6. Thiamine is shown in stick representation and colored according to the following color code: C: dark green, O: red, N: blue, S: yellow. This color code for the oxygen, nitrogen, and sulfur atoms is maintained throughout the article. C) Close-up of the substrate-binding pocket of ThiT with surface and secondary-structure representation. The surface of the L1 loop between helices 1 and 2 is colored light blue, whereas the remainder of the surface is shown in gray. Residue Trp34 is shown in dark blue and stick representation, and thiamine is represented as in (B). D) The residues involved in the binding of thiamine are shown in stick representation with their carbon atoms colored gray, whereas the other atoms and thiamine are colored as in (B). The names of the residues are given by the three-letter codes for amino acids. The dashed lines indicate electrostatic interactions and hydrogen bonds, and the gray spheres represent water molecules. Figure 1 B–D was generated with Pymol and use of chain A of structure PDB ID: 3RLB.<sup>[11]</sup>

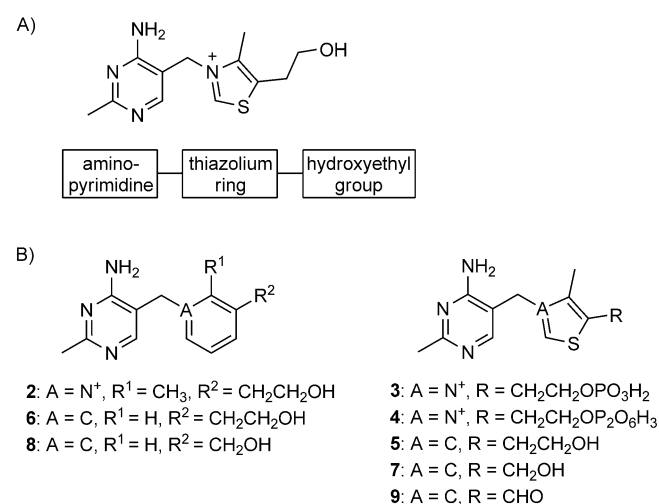
states, in order to provide new insights into the mechanism of binding and transport. Furthermore, because the ECF transporter for thiamine is essential for the uptake of this vitamin in some pathogenic bacteria, this study is a first step on the way to new antibiotics capable of blocking thiamine transport and thereby interfering with essential cellular processes within these bacteria.

## Results

### Design of small-molecule modulators

The crystal structure of ThiT in complex with thiamine (1; PDB ID: 3RLB) shows that the protein consists of six transmembrane helices (Figure 1B).<sup>[11]</sup> The substrate-binding pocket is located on the extracytoplasmic side of the membrane and is formed by residues in helices 4–6 and residues in loops L1 and L3, which are located between helices 1 and 2 and helices 3 and 4, respectively. The flexible L1 loop shields the substrate-binding pocket from the surrounding solvent in a lid-like manner, with Trp34 playing a major role in the substrate occlusion (Figure 1C).<sup>[12]</sup> The substrate-binding site is connected to the exterior of the protein through an opening of 7–9 Å in diameter, which provides multiple interaction sites for extended small molecules. Thiamine interacts with several residues in the binding pocket (Figure 1D and Figure S1 in the Supporting Information): the aminopyrimidine moiety acts as an anchor involved in hydrogen bonds with residues Glu84, His125, Tyr146, and Asn151, as well as in a  $\pi$ - $\pi$ -stacking interaction with Trp133. The thiazolium ring is engaged in  $\pi$ - $\pi$ -stacking and cation- $\pi$  interactions with Trp34 and His125, and the positively charged nitrogen atom is stabilized by an ionic interaction with Glu84. The hydroxy group forms a hydrogen bond with Tyr85. We designed small molecules and tested their ability to interact with ThiT in order to determine which functional groups are crucial for high-affinity binding (Scheme 1). MOLOC software<sup>[13]</sup> was used for molecular modeling, and the preferred orientations of the molecules in the binding pocket and the estimated free energies of binding were obtained by use of the FlexX docking module<sup>[14]</sup> and the scoring function HYDE<sup>[15,16]</sup> in the LeadIT suite, respectively.

It has previously been reported that when the thiazolium ring of thiamine (1) is substituted by a pyridinium ring, as in 2,



**Scheme 1.** Small-molecule binders for ThiT. A) Structure of thiamine (1), with the names of the rings and the hydroxyethyl group indicated. B) Structures of pyriothiamine (2), thiamine monophosphate (3), thiamine diphosphate (4), and the designed and synthesized small molecules 5–9.

**Table 1.** Binding affinities of ThiT for various small molecules as determined in the ligand-binding assay, with the errors indicated as standard deviations, together with the experimentally measured and estimated Gibbs free energies of binding ( $\Delta G$ ). The estimated values are based on the scoring function HYDE.

Compound	$K_D \pm \text{S.D. [nM]}$	$\Delta G_{\text{exp}} [\text{kJ mol}^{-1}]$	$\Delta G_{\text{est}} [\text{kJ mol}^{-1}]$
1	$0.122 \pm 0.013^{[9]}$	-57	-53
2	$0.180 \pm 0.070^{[9]}$	-56	-54
3	$1.01 \pm 0.14^{[9]}$	-51	-50
4	$1.60 \pm 0.00^{[9]}$	-50	-52
5	$4.23 \pm 1.69^{[a]}$	-48	-52
6	$266 \pm 131^{[b]}$	-38	-48
7	$5.21 \pm 3.19^{[c]}$	-47	-46
8	$528 \pm 135^{[c]}$	-36	-43
9	$7.44 \pm 1.67^{[c]}$	-46	-40

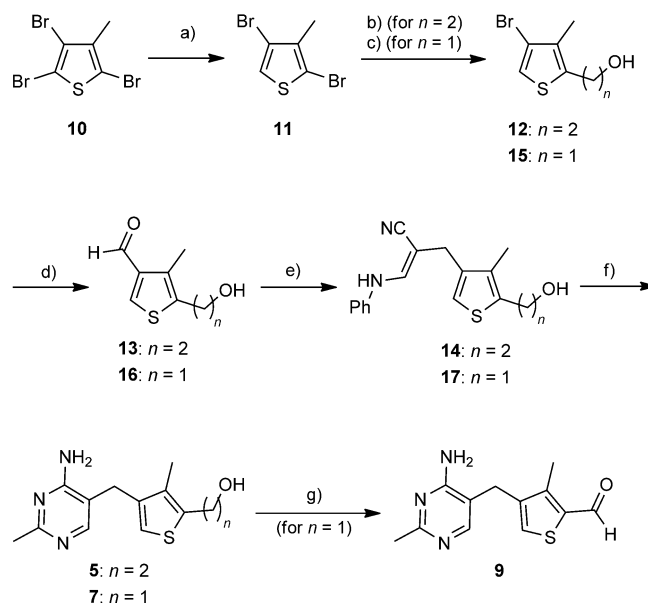
[a] The error represents the standard deviation, obtained from four experiments. [b] The error represents the standard deviation, obtained from three experiments. [c] The errors each represent the range of the data from two experiments.

the affinity of the new molecule for ThiT is essentially the same (Table 1).<sup>[9]</sup> When the hydroxy group from the hydroxyethyl side chain is mono- or diphosphorylated (compounds 3 and 4), the binding affinity decreases by one order of magnitude (Table 1).<sup>[9]</sup> Firstly, we performed docking studies for compounds 1–4, for which the  $K_D$  values had been determined previously, to benchmark how well the docking program performs on our target protein and class of compounds. According to the estimated Gibbs free energies of binding ( $\Delta G_{\text{est}}$ ), we could predict that compounds 1 and 2 should have higher binding affinities for ThiT than compounds 3 and 4, and this matched with the experimental data obtained from intrinsic-fluorescence titration assays (Table 1).

In our design, we maintained the aminopyrimidine moiety of thiamine in order to preserve the interactions between this part of the molecule and ThiT. We explored different modifications in the rest of the molecule: the thiazolium ring and the hydroxyethyl side chain. We substituted the thiazolium ring with different aromatic moieties, such as a thiophenyl (compound 5) or a phenyl ring (compound 6), to evaluate the effect on the  $\pi$ - $\pi$ -stacking interaction of this moiety with residues Trp34 and His125. In order to analyze the importance of the hydroxyethyl side chain of thiamine (1), we designed derivatives of 5 and 6 featuring either a hydroxymethyl side chain (compounds 7 and 8) or an aldehyde group (compound 9) to evaluate the importance of the hydrogen bond with Tyr85. The predicted binding poses of the new derivatives (Figure S2 in the Supporting Information) are almost identical to that of thiamine, with differences only in the hydrogen bonds formed by the new groups introduced in place of the hydroxyethyl substituent of thiamine.

### Synthesis of small-molecule modulators

Compound 5 was synthesized by optimizing a previously reported synthetic route (Scheme 2).<sup>[17]</sup> On starting from 2,3,5-tribromo-4-methylthiophene (10), after treatment with *s*BuLi and

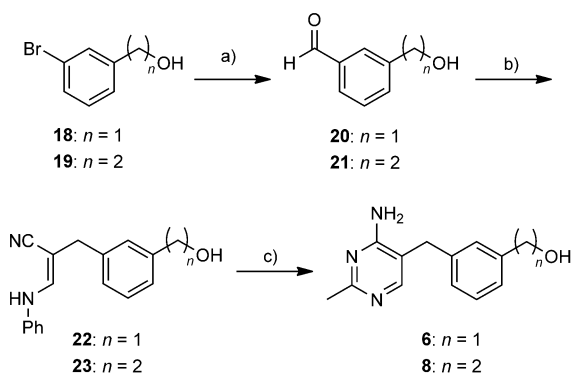


**Scheme 2.** Synthesis of compounds 5, 7, and 9. a) *s*BuLi, Et<sub>2</sub>O, -78 °C, 5 min, 93%; b) i: *s*BuLi, Et<sub>2</sub>O, -78 °C, 1 h, ii: ethylene oxide, BF<sub>3</sub>·Et<sub>2</sub>O, -78 °C to room temperature, 2 h, 68%; c) i: *s*BuLi, Et<sub>2</sub>O, -78 to -45 °C, 1 h, ii: DMF, -78 °C to RT, 2 h, iii: NaBH<sub>4</sub>, MeOH, RT, 1 h, 79% over two steps; d) i: *i*PrMgCl, THF, 0 °C, 10 min, ii: *t*BuLi, -78 to -40 °C, 1 h, iii: DMF, -78 °C to RT, 16 h, 65% (13) and 62% (16); e) 3-anilinopropionitrile, NaOEt, DMSO, microwave, 70 °C, 30–90 min, 71% (14 and 17); f) acetamidine-HCl, NaOEt, EtOH, reflux, 1–3 d, 68% (5) and 61% (7); g) MnO<sub>2</sub>, DMF, RT, 2 h, 70%.

quenching with methanol, intermediate 11 was obtained in 93% yield. In the second step, the hydroxyethyl side chain was introduced by treatment with *s*BuLi followed by reaction of the resulting anion with ethylene oxide, affording the desired product 12 in 68% yield. In the third step, treatment with *i*PrMgCl (for the in situ protection of the hydroxy group), followed by *t*BuLi, afforded an anion, which was treated with DMF to yield the aldehyde 13 (65%).<sup>[18]</sup> This aldehyde was condensed with 3-anilinopropionitrile, affording 14 in 71% yield. The aminopyrimidine ring was formed by cyclization of the enamine 14 with acetamidine under basic conditions, affording the desired product in 68% yield. Compound 5 was obtained in 21% overall yield, an improvement on the 11% overall yield reported previously.<sup>[17]</sup>

Compound 7 was synthesized by the same route. In this case, in the second step 11 was treated with *s*BuLi, and the resulting anion was allowed to react with DMF, affording an aldehyde that was reduced to the corresponding alcohol 15 with NaBH<sub>4</sub> in 79% yield over two steps. Compound 9 was obtained by oxidation of 7 with MnO<sub>2</sub>, which afforded the desired product in 70% yield.

Compounds 6 and 8 were synthesized by an analogous route (Scheme 3), and by modification of a previously reported synthesis of 8.<sup>[19]</sup> Commercially available bromides 18 and 19 were converted into the corresponding aldehydes by treatment with *i*PrMgCl, *t*BuLi, and DMF, in 74 and 70% yield for 20 and 21, respectively. These aldehydes were each condensed with 3-anilinopropionitrile under basic conditions to afford 22 and 23, in 45 and 24% yield, respectively. The final step,



**Scheme 3.** Synthesis of compounds **6** and **8**. a) i: *i*PrMgCl, THF, 0 °C, 10 min, ii: *t*BuLi, –78 to –40 °C, 1 h, iii: DMF, –78 °C to RT, 16 h, 74 % (**20**) and 70 % (**21**); b) 3-anilinopropionitrile, NaOEt, DMSO, 40 °C, 16 h, 45 % (**22**) and 24 % (**23**); c) acetamidine-HCl, NaOEt, EtOH, reflux, 1–2 d, 66 % (**6**) and 61 % (**8**).

the cyclization of the enamines **22** and **23** with acetamidine, afforded the desired products **6** and **8** in 66 and 61 % yield, respectively.

#### Ligand-binding measurements by an intrinsic-fluorescence titration assay

We determined the  $K_D$  values for compounds **5–9** by monitoring the intrinsic protein fluorescence upon addition of ligand (Table 1). The  $K_D$  values for compounds **1–4** had been determined by the same method in a previous study.<sup>[9]</sup> Replacement of the positively charged nitrogen atom in the thiazolium ring of thiamine (**1**) by a carbon atom in **5** resulted in an increase in  $K_D$  to 4.23 nM. Replacement of the thiazolium ring of **1** by a phenyl ring in compound **6** led to a decrease in binding affinity, resulting in a  $K_D$  of 266 nM. Variations of the hydroxyethyl side chain of **5** did not have any significant effect, as shown by the  $K_D$  values of 5.21 and 7.44 nM for compounds **7** and **9**, respectively. Shortening the hydroxyethyl side chain in compound **6** by one carbon atom in compound **8** led to an increase in  $K_D$  up to 528 nM.

#### Co-crystallization of ThiT with small-molecule modulators and structure determination

To visualize how the small molecules bind to ThiT, we performed co-crystallization of substrate-free ThiT (purified in 0.35 % (*w/v*) *n*-nonyl  $\beta$ -D-glucopyranoside (NG)) in the presence of various concentrations of compounds **2** and **5–9** (Table 2), at 5 °C by the vapor diffusion hanging drop method. All crystals were obtained under the same conditions as for ThiT with thiamine, with use of a reservoir solution of 0.15 M  $\text{NH}_4\text{NO}_3$  and 20 % (*w/v*) PEG 3350. The crystals grew to full size in one to two weeks and had the symmetry of space group  $C_2$ . All structures were solved to 2.0–2.5 Å resolution (Table 2). The data processing and refinement statistics are shown in Table S1 in the Supporting Information.

A comparison of the overall crystal structures of ThiT complexed to the synthesized compounds with the structure of

**Table 2.** Conditions for co-crystallization of ThiT with small-molecule binders and diffraction results.

Compound	Concentration <sup>[a]</sup> [ $\mu\text{M}$ ]	Resolution of crystal structure [Å]	RMSD alignment [Å]	
			chain A	chain B
<b>2</b>	100	2.1	0.282	0.276
<b>5</b>	10	2.5	0.341	0.322
<b>6</b>	40	2.0	0.310	0.379
<b>7</b>	10	2.2	0.305	0.274
<b>8</b>	10	2.4	0.332	0.361
<b>9</b>	10	2.2	0.287	0.317

[a] For purification and crystallization.

ThiT in complex with thiamine revealed very subtle differences only in the spatial orientations of the  $\alpha$ -helices. As in the case of ThiT complexed with thiamine, two molecules of ThiT (chains A and B) were present in the unit cell, binding one small molecule each. Comparison of the binding sites in the different chains showed only slight differences in the orientations of water molecules, except for the structures with compounds **6** and **8**. Superposition of the six structures with the corresponding chain of ThiT in complex with thiamine gave RMSD values between 0.274 and 0.379 Å, indicating that they are almost identical (Table 2). When zooming into the residues of ThiT involved in substrate binding, we noticed significant changes in the orientations of the side chains only for Trp34 in the complexes with compounds **6** and **8**. Figure 2A–F shows the binding site residues in chain A of ThiT co-crystallized with compounds **2** and **5–9**, respectively. The binding sites in chain B of ThiT are shown in Figure S3. The  $\pi$ – $\pi$ -stacking interactions of the thiazolium ring sandwiched between Trp34 and His125 are conserved in most of the co-crystallized structures, as we predicted (Figure S2). In the co-crystallized structures with compounds **6** and **8**, Trp34 has moved in the direction of the pyrimidine ring, making a CH– $\pi$  interaction with this ring. In the binding site of compound **6** in chain B of the structure (Figure S3D), Trp34 is located even further away from the pyrimidine ring, making it possible for a PEG molecule to bind nonspecifically in the binding pocket. In the case of compound **8**, Trp34 is in a position similar to that in the structure of ThiT in complex with thiamine in the binding site in chain A (Figure 2E). However, the electron density for this residue extends to the side of the pyrrole moiety of the indole, showing that it could also adopt the position shown in the binding site in chain B (Figure S3F).

Despite the movement of the side chain of Trp34 and the broadening of the entrance to the binding pocket in the cases of these two compounds, the backbone of the L1 loop maintains its position. The electrostatic interaction of Glu84 with the positively charged nitrogen atom in the thiazolium ring is only conserved in the complex with compound **2**, this being the only derivative in which the charged nitrogen atom is maintained. The hydroxyethyl group of compound **5** forms water-mediated hydrogen bonds with Asn29 and Tyr85. The same group of compound **6** forms hydrogen bonds through a single molecule of water with both Tyr85 and His72. The hydroxymethyl or aldehyde groups of compounds **7** and **9** form

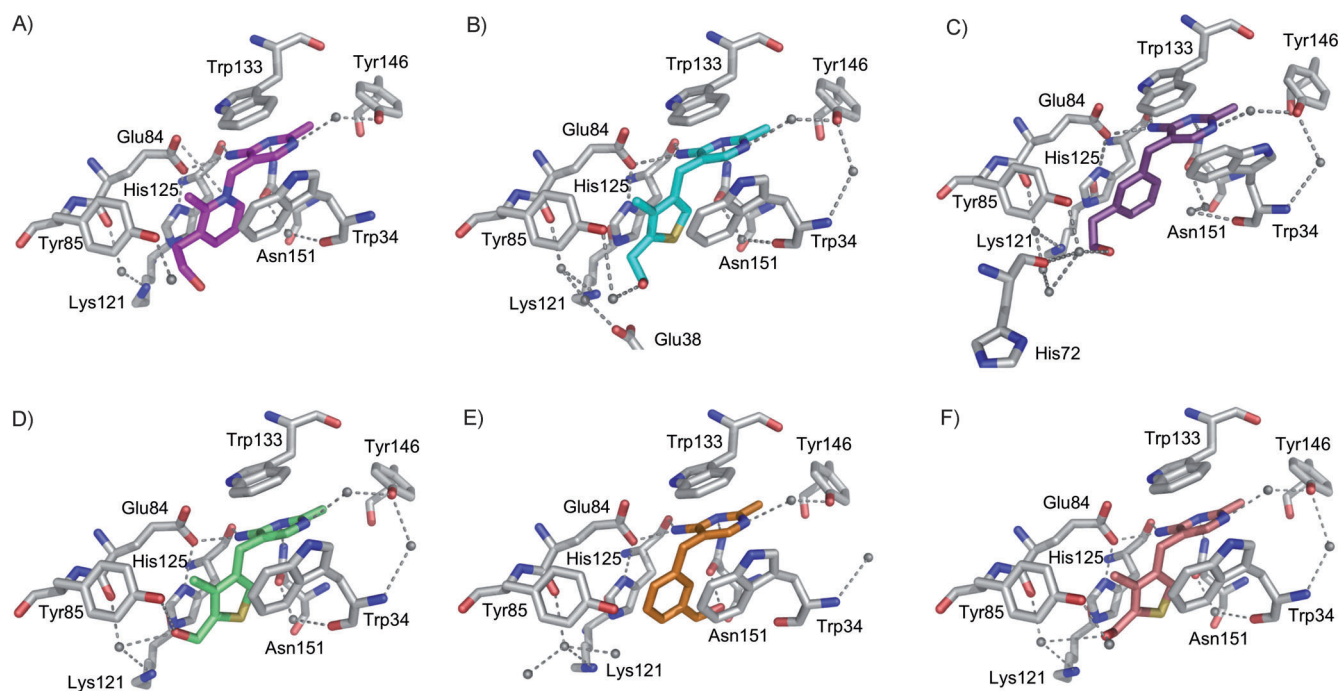


**Figure 2.** Co-crystal structures of ThiT with small-molecule binders. The residues involved in the binding of the small-molecule binders are shown with use of the same format and color code as in Figure 1 D. A)–F) The carbon atoms of compounds **2** and **5–9** are shown in magenta (PDB ID: 4MUU), cyan (4MHW), violet purple (4MES), lime (4POV), orange (4N4D), and deep salmon (4POP), respectively. The figure was created by using chain A of the corresponding PDB file.

water-mediated hydrogen bonds with the backbone carbonyl group of Glu84, the amino group of Lys121, and the hydroxy group of Tyr85. In the case of compound **8**, the phenyl ring has flipped over, relative to its position for compound **6**, so as to allow the hydroxymethyl group to form a direct hydrogen bond with the backbone carbonyl group of Asn151. Besides the ordered water molecule through which Tyr146 interacts with the pyrimidine ring of the ligands, there are a few other water molecules involved in connecting binding site residues with each other. The side chain of Lys121 interacts with the backbone of Glu84 through an ordered water molecule in all structures, which likely assures correct alignment of His125 with the ligand. In addition, the backbone of Trp34 makes interactions with the side chains of Tyr146 and Asn151 through ordered water molecules; this could help the backbone of loop L1 to keep its position.

## Discussion

We have studied the binding of thiamine derivatives to ThiT, the S-component for thiamine in *L. lactis*, by modifying moieties of thiamine in a modular manner. Because the crystal structure of ThiT features promising pockets for expansion of thiamine adjacent to the thiazolium ring and the hydroxyethyl side chain, we focused on modifications of these moieties whilst keeping the pyrimidine moiety intact. The estimated  $\Delta G$  values ( $\Delta G_{\text{est}}$ ) from the docking studies correlate very well with the experimentally measured  $\Delta G$  values derived from the  $K_D$  measurements by intrinsic-fluorescence titration ( $\Delta G_{\text{exp}}$ ). In addition, the binding poses observed by X-ray crystallography

are in agreement with those predicted with computational methods, thus highlighting the power of docking studies when probing protein–ligand interactions.

From the  $K_D$  values obtained from the intrinsic-fluorescence titration measurements, we conclude that the presence of the positively charged nitrogen atom in the central ring contributes to the picomolar binding affinity. Compounds **1** and **2**, in which the thiazolium ring is replaced by a pyridinium ring, display comparable  $K_D$  values of 122  $\mu\text{M}$  and 180  $\mu\text{M}$ , respectively. Measuring  $K_D$  values in the low nanomolar or picomolar range with high accuracy is difficult, and with a ThiT concentration of 50 nM in the intrinsic-fluorescence titration assay, these values cannot be considered significantly different. Replacement of the thiazolium ring by a thiophene ring, and thereby removing the positive charge, lowered the binding affinity about 30-fold. Nonetheless, derivatives **5**, **7**, and **9** still bind with high affinity to ThiT ( $K_D$  values between 4.2 and 7.4 nM), showing that these analogues are suitable thiamine mimics. Removal of the positively charged nitrogen atom and the methyl group in compounds **6** and **8**, relative to **2**, led to decreases in binding affinity, resulting in  $K_D$  values in the upper nanomolar range. This indicates that the presence of the charged nitrogen atom in the context of a six-membered ring provides a bigger contribution to interactions involved in binding than in the case of the five-membered ring. From the co-crystallization studies we could see that Glu84 is engaged in an electrostatic interaction with the positively charged nitrogen atom, and that this is lost when this nitrogen is missing. In addition, the charged nitrogen atom also enables cation– $\pi$  interactions with Trp34 and His125. In the absence of the charged nitrogen, only  $\pi$ – $\pi$

stacking interactions can be formed, resulting in a weaker interaction of the ligand with Trp34 and His125. In the cases of co-crystallization with compounds **6** and **8**, Trp34 was displaced in the direction of the pyrimidine ring, leaving only His125 to form  $\pi$ - $\pi$ -stacking interactions with the phenyl ring in these compounds. Both changes decreased the binding affinities, with  $K_D$  values of 266 and 528 nM for compounds **6** and **8**, respectively.

On comparing compounds **5** and **7**, each featuring a thiophenyl ring, with compounds **6** and **8**, each with a phenyl ring, the binding affinity is about 50 to 70 times lower in the case of the phenyl ring. The difference in affinity could be explained by the sulfur atom in compounds **5** and **7**, which can engage in S- $\pi$  interactions with Trp34 and His125, and by the methyl group at C-4, which could also contribute through CH- $\pi$  interactions with Tyr85. Furthermore, different alignments of the dipole moments of the aromatic moieties could also account for the observed difference in affinity. Removing the methyl group in compounds **6** and **8** leads to a loss of van der Waals interactions. In the cases of these two compounds, the side chain of Trp34 adopts conformations different from those in the other co-crystal structures; this could also be a reason for the drop in binding affinity.

Having investigated the importance of the central ring, we next examined the importance of the hydrogen-bonding interaction with Tyr85. To do this, we modified the hydroxyethyl group in compounds **7**–**9**. Compound **7** shows that shortening the spacer by one carbon atom to a hydroxymethyl group does not change the binding affinity significantly relative to compound **5**. In the cases of compounds **6** and **8**, the same shortening increases the  $K_D$  values roughly twofold. In the case of compound **8**, the interaction with Tyr85 is lost and instead, a new hydrogen bond is formed with the carbonyl group of Asn151. This carbonyl group is in closer proximity than Tyr85, but the interaction with Asn151 does not seem to contribute to the binding affinity to the same degree as an interaction with Tyr85. In addition, compound **8** also interacts with the backbone carbonyl group of Trp34 through an ordered water molecule. The lack of interactions between compound **8** and residues Glu84, Tyr85, and Lys121 through an ordered water network might weaken binding, thereby lowering the binding affinity to a larger extent relative to the binding affinity of compound **6**. The interaction of the aldehyde group of compound **9** with Tyr85 appears to contribute to the binding affinity almost as well as that of the hydroxyethyl group in compound **5**, so there is no real preference for a hydrogen bond donor or acceptor on this side of the substrate, given that most interactions between the ligands and Tyr85 are water-mediated. In addition, in the binding site in chain B of ThiT in complex with thiamine (Figure S3A), the hydroxyethyl group of thiamine has turned away from Tyr85 and is now engaged in a hydrogen bond with the side chain of Glu38. This indicates that the interaction between Tyr85 and the ligand is not particularly important and does not make a major contribution to the high-affinity binding.

## Conclusions

At the outset of this study, we hypothesized that the designed thiamine derivatives might trap ThiT in previously undetected conformational states, and that this might allow us to follow the changes in conformation that take place for substrate binding and release. Surprisingly, in spite of differences in affinity of over three orders of magnitude (compounds **1** and **8**) the crystal structures of ThiT with the bound thiamine derivatives were almost identical. The only difference in the binding-site residues that we observed is a rotation of the side chain of Trp34 located in loop L1 when compounds **6** and **8** are bound. The different orientation of Trp34 opens the entrance to the binding site pocket slightly, but the backbone of loop L1 maintains its position, keeping the substrate-binding pocket intact. Although this observation is consistent with the EPR studies on ThiT that showed that the main structural difference between apo-ThiT and the thiamine-bound protein is the conformation of loop L1,<sup>[12]</sup> it does not provide the anticipated mechanistic insight into the mechanism of binding. Apparently, the structure of the binding site in the S-component is so robust that it stays intact, even if lower-affinity substrates bind. This robustness has direct consequences for the transport mechanism employed by the ECF transporter. We hypothesize that the S-component “topples” in the membrane only if the loop L1 is closed. Interaction with the ECF module is required for “toppling”, resulting in the exposure of the binding site to the cytoplasmic side of the membrane, where the substrate can be released. Possibly ATP hydrolysis is needed for opening of the binding site and substrate release. Indeed, in the context of the entire complex (S-component and ECF module), the substrate-binding site of the S-component FoIT (for folate) is disrupted and the loop L1 is displaced outward.<sup>[6]</sup> We speculate that a substantial input of free energy is required to accomplish the changes in conformation in the S-component's binding site that are necessary for transport and release of the substrate. This energy is probably provided by the association with the ECF module and by binding and hydrolysis of ATP by the NBDs.

The observation that the thiamine derivatives bind to ThiT with high affinities is very promising for another reason. It suggests that the versatile scaffold of the derivatives that lack the thiazolium ring (compounds **5**, **7**, and **9**) could be further modified, which is an important step in the design of new derivatives. They can assist not only in the elucidation of the transport mechanism but also in the development of new antibiotics targeted against pathogenic bacteria that depend on this type of transporters.

## Experimental Section

**Materials:** The detergents *n*-dodecyl  $\beta$ -D-maltopyranoside (DDM), *n*-decyl  $\beta$ -D-maltopyranoside (DM), and NG were purchased from Anatrace. All reagents used for the synthesis of the small-molecule modulators were purchased from Sigma-Aldrich, Acros Organics, or TCI Europe, and were used without further purification unless

noted otherwise. All solvents were reagent-grade and, if necessary, dried and distilled prior to use.

**Modeling and docking of small-molecule modulators:** The crystal structure of ThiT in complex with thiamine (PDB ID: 3RLB) was used for modeling.<sup>[11]</sup> Thiamine derivatives were designed by using the program MOLOC,<sup>[13]</sup> and the energy of the system was minimized by use of the MAB force field implemented in this software, while the protein coordinates and the crystallographically localized water molecule (HOH196) were kept fixed. Hydrogen bonds and hydrophobic interactions were measured in MOLOC. The designed thiamine derivatives were subsequently docked into the binding pocket of ThiT with the aid of the FlexX docking module in the LeadIT suite.<sup>[14]</sup> During docking, the binding site in the protein was restricted to 8.0 Å around the co-crystallized thiamine, and the 30 top-scored solutions were retained and subsequently post-scored with the scoring function HYDE.<sup>[15,16]</sup> After careful visualization to exclude poses with significant inter- or intramolecular clash terms or unfavorable conformations, the resulting solutions were subsequently ranked according to their binding energies.

**Synthesis of small-molecule modulators—general methods:** All reactions were carried out under nitrogen (if not otherwise indicated), with use of dried glassware. Reactions were monitored either by GC-MS (GCMS-QP2010 Shimadzu) with a HP-5 column (Agilent Technologies) or by thin-layer chromatography (TLC) on silica-gel-coated aluminium foils (silica gel 60/Kieselguhr F254, Merck). Flash-column chromatography was performed on silica gel (SiliCycle 40–63 µm). Melting points were determined with a Büchi B-545 apparatus. NMR spectra were recorded with a Varian AMX 400 spectrometer at 25 °C. Chemical shifts ( $\delta$ ) are reported in ppm relative to the residual solvent peak. FTIR spectra were measured with a PerkinElmer FTIR spectrometer. High-resolution mass spectra were recorded with a Thermo Scientific LTQ Orbitrap-XL mass spectrometer. Details of the synthesis and characterization are described in the Supporting Information.

**Expression and purification of ThiT:** Expression of native ThiT with N-terminal His<sub>8</sub>-tag was performed as described previously,<sup>[9,11]</sup> with some modifications. Briefly, *L. lactis* NZ9000 cells<sup>[20]</sup> with *pNZnHisThiT* plasmid were grown semi-anaerobically in chemically defined medium<sup>[21]</sup> without thiamine and supplemented with glucose (2.0%, w/v) and chloramphenicol (5 µg mL<sup>-1</sup>) in a 10 L bioreactor at 30 °C and pH 6.5. At an OD<sub>600</sub> of 1.5, expression of ThiT was induced by addition of culture supernatant (0.1%, v/v) from a Nisin-A-producing strain.<sup>[20]</sup> The cells were induced for 3 h and harvested at a final OD<sub>600</sub> of 7–8. After harvesting and washing by centrifugation for 15 min at 6000 rpm (JLA9.1000 rotor) and 4 °C, the cells were resuspended in buffer A [potassium phosphate buffer (KPi, pH 7.0, 50 mM)], frozen in liquid nitrogen, and stored at –80 °C.

The preparation of membrane vesicles was performed as described previously,<sup>[9]</sup> with some modifications. After the resuspended cells had been thawed, MgSO<sub>4</sub> (5 mM) and DNase (375 µg mL<sup>-1</sup>) were added. The cells were lysed by high-pressure disruption (Constant Cell Disruption Systems, Ltd, UK, twofold passage at 269 MPa and 4 °C), and the cell debris was separated from the membrane vesicles by low-speed centrifugation for 30 min at 15000 rpm (JA25.50 rotor) and 4 °C. The membrane vesicles were harvested by high-speed centrifugation for 2 h at 40000 rpm (45Ti rotor) and 4 °C, resuspended in buffer A to a final concentration of 10 mg mL<sup>-1</sup>, frozen in liquid nitrogen, and stored at –80 °C.

For the purification of substrate-free ThiT, membrane vesicles were rapidly thawed and resuspended in buffer B [KPi (pH 7.0, 50 mM),

KCl (200 mM), glycerol (10%, w/v)] to a final concentration of 6–10 mg mL<sup>-1</sup>. For the ThiT co-crystallization experiments, certain concentrations of compounds **2** and **5–9** (Table 2) were added to all buffers used during the purification. The membrane vesicles were solubilized with DDM (1%, w/v) for 1 h at 4 °C with gentle rocking. The undissolved material was removed by centrifugation for 30 min at 80000 rpm (MLA-80 rotor) and 4 °C. The supernatant was incubated with Ni<sup>2+</sup>-Sephacrose resin (column volume = 0.5 mL), equilibrated with buffer B, for 1 h at 4 °C with gentle rocking. Subsequently, the suspension was poured onto a 10 mL disposable column (Bio-Rad) and, after collection of the flow-through, the column material was washed with 20 column volumes of buffer C [KPi (pH 7.0, 50 mM), KCl (200 mM), imidazole (50 mM), DM (0.15%, w/v)]. In cases of purification of protein for crystallization, DM was replaced with NG (0.35%, w/v). The protein was eluted in three fractions (of 350, 650, and 500 µL) of buffer D (KPi (pH 7.0, 50 mM), KCl (200 mM), imidazole (500 mM), DM (0.15%, w/v)). In cases of purification of protein for crystallization, DM was replaced with NG (0.35%, w/v). EDTA (1 mM) was added to the second elution fraction, which contained most of the purified protein, and this fraction was loaded on a Superdex 200 10/300 gel filtration column (GE Healthcare) equilibrated with buffer E [KPi (pH 7.0, 50 mM), KCl (150 mM), DM (0.15%, w/v)]. In cases of purification of protein for crystallization, buffer F [HEPES (pH 7.0, 20 mM), KCl (150 mM), NG (0.35%, w/v)] was used for gel-filtration chromatography. After gel-filtration chromatography, the fractions containing ThiT were used directly for further analysis or concentrated by use of a Vivaspin 2 concentrator device with a molecular weight cut-off of 50 kDa (Sartorius stedim) to a final concentration of 6–10 mg mL<sup>-1</sup> and used for crystallization.

**Ligand-binding measurements by intrinsic-fluorescence titration assay:** The ligand-binding measurements by intrinsic-fluorescence titration were performed as described previously,<sup>[9]</sup> by use of a Spec Fluorlog 322 fluorescence spectrophotometer (Jobin Yvon), with some modifications. Purified ThiT was diluted in buffer E to a concentration of about 50 nM in a final volume of 800 µL. The substrates were added in 1 µL steps from a Harvard apparatus syringe pump with a 500 µL gas-tight glass syringe (Hamilton). With use of an excitation wavelength of 280 nm, emission was measured at 350 nm and 25 °C. After each addition of substrate, 10 s were allowed for equilibration and mixing, and the signals were averaged over 15 s. The data analysis was performed as described.<sup>[9]</sup>

**Co-crystallization of ThiT with small-molecule modulators and structure determination:** The concentrated ThiT (purified in NG (0.35%, w/v)) in the presence of compounds **2** or **5–9** (see Table 2 for the concentrations used) was used to set up 24-well hanging drop crystallization plates with use of a reservoir solution (NH<sub>4</sub>NO<sub>3</sub> (0.15 M), PEG 3350 (20%, w/v)). Hanging drops of 2 µL were set up in a 1:1 ratio of concentrated protein solution to reservoir solution. The plates were incubated at 5 °C, and after one to two weeks, crystals appeared. For cryoprotection, a cryoprotection solution (NH<sub>4</sub>NO<sub>3</sub> (15 mM), PEG 3350 (40% or 50%, w/v)) was used when the crystals were fished. Diffraction data were collected at the DESY, Hamburg (ThiT co-crystallized with compounds **6**, **7**, or **9**) or the ESRF, Grenoble (ThiT co-crystallized with compounds **2**, **5**, or **8**). Data processing was carried out by use of XDS,<sup>[22]</sup> and molecular replacement was performed with the aid of Phaser MR in the CCP4 suite,<sup>[23]</sup> with use of the structure of thiamine-bound ThiT (PDB ID: 3RLB).<sup>[11]</sup> Refinements were performed by use of both Phenix refinement<sup>[24]</sup> and Refmac.<sup>[25]</sup> Manual model building and the placement of substrate, detergent, and PEG molecules were done with

Coot.<sup>[26]</sup> Refinement statistics are shown in Table S1. The crystal structures were deposited in the PDB with the following PDB IDs. ThiT + compound 2: 4MUU. ThiT + compound 5: 4MHW. ThiT + compound 6: 4MES. ThiT + compound 7: 4POV. ThiT + compound 8: 4N4D. ThiT + compound 9: 4POP.

## Acknowledgements

The research leading to these results has received funding from the European Community's Seventh Framework Programme (FP7/2007–2013) under BioStruct-X (grant agreement N°283570), the Ministry of Education, Culture and Science (Gravitation program 024.001.035), the Netherlands Organisation for Scientific Research (NWO) (NWO ChemThem grant 728.011.104 and NWO Vici grant 865.11.001), and the European Research Council (ERC) (ERC Starting Grant 282083). The Deutsches Elektronen-Synchrotron (DESY) and the European Synchrotron Radiation Facility (ESRF) are acknowledged for beam line facilities.

**Keywords:** energy-coupling factor transporter · membrane proteins · molecular recognition · structure-based design · X-ray diffraction

- [1] J. ter Beek, A. Guskov, D. J. Slotboom, *J. Gen. Physiol.* **2014**, *143*, 419–435.
- [2] D. J. Slotboom, *Nat. Rev. Microbiol.* **2014**, *12*, 79–87.
- [3] D. A. Rodionov, P. Hebbeln, A. Eudes, J. Ter Beek, I. A. Rodionova, G. B. Erkens, D. J. Slotboom, M. S. Gelfand, A. L. Osterman, A. D. Hanson, T. Eitinger, *J. Bacteriol.* **2009**, *191*, 42–51.
- [4] T. Eitinger, D. A. Rodionov, M. Grote, E. Schneider, *FEMS Microbiol. Rev.* **2011**, *35*, 3–67.
- [5] C. T. Jurgenson, T. P. Begley, S. E. Ealick, *Annu. Rev. Biochem.* **2009**, *78*, 569–603.
- [6] K. Xu, M. Zhang, Q. Zhao, F. Yu, H. Guo, C. Wang, F. He, J. Ding, P. Zhang, *Nature* **2013**, *497*, 268–271.
- [7] T. Wang, G. Fu, X. Pan, J. Wu, X. Gong, J. Wang, Y. Shi, *Nature* **2013**, *497*, 272–276.
- [8] M. Zhang, Z. Bao, Q. Zhao, H. Guo, K. Xu, C. Wang, P. Zhang, *Proc. Natl. Acad. Sci. USA* **2014**, *111*, 18560–18565.
- [9] G. B. Erkens, D. J. Slotboom, *Biochemistry* **2010**, *49*, 3203–3212.
- [10] R. Kluger, K. Tittmann, *Chem. Rev.* **2008**, *108*, 1797–1833.
- [11] G. B. Erkens, R. P. Berntsson, F. Fulyani, M. Majsnerowska, A. Vujičić-Žagar, J. Ter Beek, B. Poolman, D. J. Slotboom, *Nat. Struct. Mol. Biol.* **2011**, *18*, 755–760.
- [12] M. Majsnerowska, I. Hänel, D. Wunnicke, L. V. Schäfer, H. J. Steinhoff, D. J. Slotboom, *Structure* **2013**, *21*, 861–867.
- [13] P. R. Gerber, K. Müller, *J. Comput.-Aided Mol. Des.* **1995**, *9*, 251–268.
- [14] *LeadIT (version 2.1.2)*, BioSolveIT, GmbH.
- [15] I. Reulecke, G. Lange, J. Albrecht, R. Klein, M. Rarey, *ChemMedChem* **2008**, *3*, 885–897.
- [16] N. Schneider, S. Hindle, G. Lange, R. Klein, J. Albrecht, H. Briem, K. Beyer, H. Claußen, M. Gastreich, C. Lemmen, M. Rarey, *J. Comput.-Aided Mol. Des.* **2012**, *26*, 701–723.
- [17] H. Zhao, L. P. S. De Carvalho, C. Nathan, O. Ouerfelli, *Bioorg. Med. Chem. Lett.* **2010**, *20*, 6472–6474.
- [18] J. Ko, J. Ham, I. Yang, J. Chin, S. J. Nam, H. Kang, *Tetrahedron Lett.* **2006**, *47*, 7101–7106.
- [19] S. Mann, C. Perez Melero, D. Hawksley, F. J. Leeper, *Org. Biomol. Chem.* **2004**, *2*, 1732–1741.
- [20] O. P. Kuipers, P. G. G. de Ruyter, M. Kleerebezem, W. M. de Vos, *J. Biotechnol.* **1998**, *64*, 15–21.
- [21] R. P. Berntsson, N. Alia Oktaviani, F. Fusetti, A.-M. W. H. Thunnissen, B. Poolman, D.-J. Slotboom, *Protein Sci.* **2009**, *18*, 1121–1127.
- [22] W. Kabsch, *Acta Crystallogr. Sect. D Biol. Crystallogr.* **2010**, *66*, 125–132.
- [23] M. D. Winn, C. C. Ballard, K. D. Cowtan, E. J. Dodson, P. Emsley, P. R. Evans, R. M. Keegan, E. B. Krissinel, A. G. W. Leslie, A. McCoy, S. J. McNicholas, G. N. Murshudov, N. S. Pannu, E. A. Potterton, H. R. Powell, R. J. Read, A. Vagin, K. S. Wilson, *Acta Crystallogr. Sect. D Biol. Crystallogr.* **2011**, *67*, 235–242.
- [24] P. D. Adams, P. V. Afonine, G. Bunkóczi, V. B. Chen, I. W. Davis, N. Echols, J. J. Headd, L.-W. Hung, G. J. Kapral, R. W. Grosse-Kunstleve, A. J. McCoy, N. W. Moriarty, R. Oeffner, R. J. Read, D. C. Richardson, J. S. Richardson, T. C. Terwilliger, P. H. Zwart, *Acta Crystallogr. Sect. D Biol. Crystallogr.* **2010**, *66*, 213–221.
- [25] G. N. Murshudov, A. A. Vagin, E. J. Dodson, *Acta Crystallogr. Sect. D Biol. Crystallogr.* **1997**, *53*, 240–255.
- [26] P. Emsley, B. Lohkamp, W. G. Scott, K. Cowtan, *Acta Crystallogr. Sect. D Biol. Crystallogr.* **2010**, *66*, 486–501.

Received: November 24, 2014

Published online on February 12, 2015